Photodissociation of the Deuteron from 150 to 450 Mev*

J. C. Keck† and A. V. Tollestrup
California Institute of Technology, Pasadena, California

(Received August 5, 1955)

The photodissociation of the deuteron has been investigated for laboratory photon energies of 150, 200, 250, 300, 350, 400, and 450 Mev at laboratory angles of 39, 56, 74, 93, 115, and 138 degrees. The process was identified by detecting the recoil protons in a range-ionization telescope. The total cross section has a relative minimum at 150 Mev followed by a relative maximum at 250 Mev where its values are 53×10^{-30} cm^2 and 63×10^{-30} cm^2, respectively. From 150 to 250 Mev the center-of-momentum angular distributions have a strong forward maximum which diminishes at higher energies until the distributions become approximately symmetrical. There is qualitative agreement with meson theories on some points.

I. INTRODUCTION

THE photodissociation of the deuteron is the simplest reaction involving the interaction of a photon with a complex nucleus. In its most general form, the theory of this process involves not only a knowledge of the electromagnetic interactions but also an understanding of the nature of nuclear forces. At low energies the details of the latter are relatively unimportant and successful calculations have been made up to about 10 Mev using the concepts of effective range theory.[1] At higher energies, as the de Broglie wavelength of the nucleons becomes comparable to the range of nuclear forces, the details of the force law become important and, in particular, effects due to meson exchange currents may begin to appear in an explicit fashion. The study of this reaction can, therefore, give valuable information on the influence of meson fields on a process in which no free mesons ever appear. Since the reaction occurs below meson threshold as well as above, we can obtain this information in an energy region forbidden to photopion production or pion-nucleon scattering experiments.

In addition to being an interesting problem in itself, the high-energy photodissociation of the deuteron may also be linked to other photoprocesses. For example, it is basic to Levinger's pseudo-deuteron model[2] of the photoelectric effect in heavier nuclei and may be used in conjunction with detailed balance to predict the n–p capture process.[3]

The first indication that the cross section for photodissociation of the deuteron might be considerably larger at high energies than that calculated for ordinary electric interactions came from experiments[4] in 1951 on photostar and photoproton production in heavier nuclei as interpreted in terms of Levinger's pseudo-deuteron theory[2] by Wilson.[5] Confirmation of a large cross section for photodissociation was almost immediately provided by direct measurements on deuterium in the energy range from 80 to 300 Mev at Berkeley[6] and Cornell.[7] Although all of the early work showed an anomalous cross section, the agreement between the different experiments was very poor. With the recent publication of a series of experiments at Illinois[8] covering the energy range from 20 to 260 Mev, which check in part the work at Cornell[9] at 180 and 260 Mev, the situation was very much improved. The present experiment covers the energy range from 100 to 450 Mev and is in good agreement with the Cornell and Illinois results in the overlapping energy region. Thus our knowledge of the cross section for the photodissociation of the deuteron now extends from threshold to 450 Mev with fair precision.

In Sec. II of this paper the experimental procedure used is outlined. We have relegated to Sec. III the discussion of some important details thought to be of interest primarily to experimenters engaged in similar work. Section IV gives an account of the reduction and correction of the data and Sec. V contains a summary of the results. Sec. VI is devoted to a discussion of the results and a comparison with existing theories.

II. EXPERIMENTAL PROCEDURE *A*

In the present experiment the process

$$\gamma+d\rightarrow p+n$$

has been studied for photon energies from 150 to 450 Mev by measuring the energy and angle of the recoil proton. In the absence of backgrounds or competing processes in deuterium, this serves as a unique identification. Backgrounds were largely eliminated by em-

* This work was supported in part by the U. S. Atomic Energy Commission.

† Now at the Everett, Massachusetts, Laboratory of the Avco Manufacturing Corporation.

[1] For a summary of low-energy work see J. Blatt and V. F. Weisskopf, *Theoretical Nuclear Physics* (John Wiley and Sons, Inc., New York, 1952).

[2] J. Levinger, Phys. Rev. **84**, 43 (1951).

[3] J. DePangher (private communication).

[4] D. Walker, Phys. Rev. **81**, 634 (1951); S. Kikuchi, Phys. Rev. **81**, 1060 (1951); R. Miller, Phys. Rev. **82**, 260 (1951); C. Levinthal and A. Silverman, Phys. Rev. **82**, 822 (1951); J. Keck, Phys. Rev. **85**, 410 (1952).

[5] R. R. Wilson, Phys. Rev. **86**, 125 (1952).

[6] S. Kikuchi, Phys. Rev. **85**, 1062 (1952); W. S. Gilbert and J. W. Rosengren, Phys. Rev. **88**, 901 (1952).

[7] T. S. Benedict and W. M. Woodward, Phys. Rev. **85**, 924 (1952); R. Littauer and J. Keck, Phys. Rev. **86**, 1051 (1952).

[8] Yamagata, Barton, Hanson, and Smith, Phys. Rev. **95**, 576 (1954); E. A. Whalin, Phys. Rev. **95**, 1362 (1954); Lew Allen, Jr., Phys. Rev. **98**, 705 (1955).

[9] Keck, Littauer, O'Neill, Perry, and Woodward, Phys. Rev. **93**, 827 (1954).

ploying a target containing pure deuterium gas. However, above the threshold for pion production, there are proton recoils associated with the processes

$$\gamma+d\rightarrow p+n+\pi^0$$
$$\gamma+d\rightarrow p+p+\pi^-,$$

and it is necessary to distinguish between these recoils and those produced in the photodissociation. This can be done on the basis of the dynamics of the reactions. For photodissociation the relation between photon energy and proton energy and angle is unique and is shown by the full curves in Fig. 1. The pion production process involves a three-body reaction and the relation between photon and proton energy is not unique. Two limiting cases are of interest, however. The first is that in which the pion is produced on one nucleon in the deuteron with no momentum transfer to the "spectator" nucleon. If we assume the struck necleon to have been initially at rest, then the dynamics of this process are just those for meson production on hydrogen and are shown by the broken curves in Fig. 1. The other case is that in which the recoil protons have the maximum energy possible, and this case corresponds to the meson and partner necleon recoiling as a unit. The curves for this process, which we shall call "apron-string" pion production, are shown as dashed lines in Fig. 1. As can now be seen, for a given end point of the bremsstrahlung spectrum, there is a range of energies lying above those for "apron-string" pion production for which photodissociation is the only possible process. At lower energies, recoil protons from pion production are

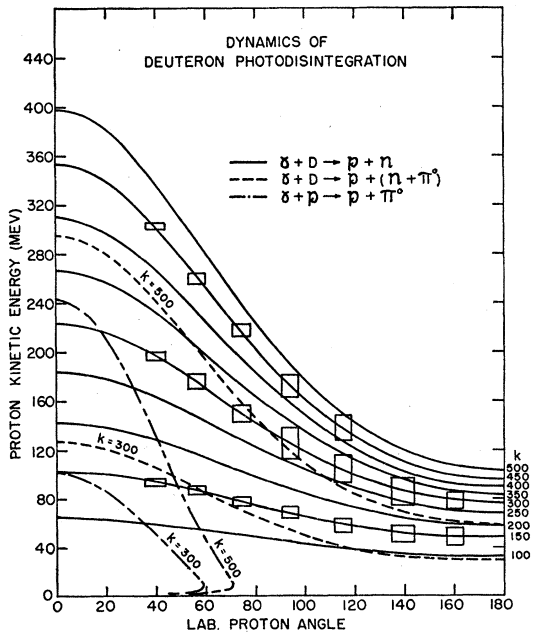

FIG. 1. Dynamics of deuteron dissociation and competing reactions. The rectangles indicate typical values of the resolution employed.

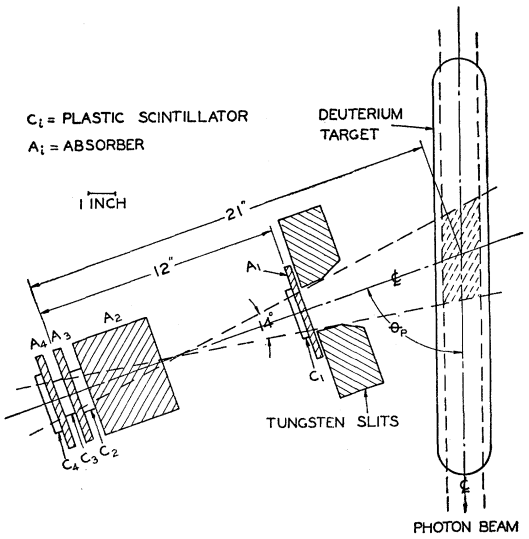

FIG. 2. Schematic of experimental arrangement. The telescope was shielded at the sides by four inches of lead not shown.

possible, but only in the region of the "spectator" process do we expect the competition from this source to be serious.[10] By progressively lowering the end-point energy of the bremsstrahlung, we can investigate the entire range for photodissociation and check on the seriousness of competition in the doubtful region.

The experimental arrangement used to study the recoil protons is shown in Fig. 2. The source of photons was the California Institute of Technology 500-Mev synchrotron. The beam was collimated to a diameter of $1\frac{1}{2}$ in. at the target by a primary lead collimator located 13 feet in front of the target. Two additional collimators having diameters slightly larger than the beam were employed to reduce the background of scattered radiation from the primary collimator. The intensity was monitored by an ionization chamber having 1-in. copper walls located behind the target. This monitor has been calibrated for 500-Mev bremsstrahlung by both a pair spectrometer[11] and a shower curve.[12] Unfortunately, the two calibrations disagree by 15%, but the adopted mean of $(4.44\pm0.32)\times10^{18}$ Mev/coulomb at S.T.P. is within 7% of a reasonable extrapolation of Cornell and Illinois calibrations made at 300 Mev.

The target was deuterium gas at 2000 psi and liquid nitrogen temperature. The vessel containing the gas was 17 in. long by 2 in. in diameter and had 30-mil steel walls. It was cooled at one end by liquid nitrogen with thermal insulation provided by $1\frac{1}{2}$ in. of styrofoam. The temperature and pressure of the target were

[10] J. Keck and R. Littauer, Phys. Rev. **88**, 139 (1952).
[11] D. Cooper, Ph.D. thesis, California Institute of Technology, 1954 (unpublished).
[12] Method of Blocker, Kenny, and Panofsky, Phys. Rev. **79**, 419 (1950).

monitored and used to determine the specific volume from the equation of state.[13]

The proton counter was a range-ionization telescope consisting normally of four plastic scintillators separated by copper absorbers. The event recorded was a coincidence between counters 1, 2, and 3 accompanied by an anticoincidence in counter 4, i.e. (1+2+3−4). This fixed the range of the particles counted between R and $R+\Delta R$ where $R\approx A_1+C_1+A_2+C_2+A_3$ and $\Delta R\approx C_3+A_4$. Protons were separated from mesons and electrons by observing their ionization in counter 1 with a differential pulse-height analyzer. The angle of observation and the solid angle of acceptance were determined by counter 3 and a tungsten slit tapered to reduce slit edge penetration and arranged to exclude protons produced in the end walls of the target. A more complete description of the telescope is given in Sec. III.

For the geometry just described which involves a cylindrical source viewed through an aperture at an angle, θ, the number of counts, N, is related to the laboratory cross section, $d\sigma/d\Omega_L$, by the expression:

$$N=\frac{d\sigma}{d\Omega_L}N_\gamma N_T\int_{\tau\Omega}d\tau d\Omega, \tag{1}$$

where N_γ is the number of photons contributing to the observed reaction, N_T is the number of target nuclei per unit volume, $d\tau$ is a differential element of target volume and $d\Omega$ is a differential element of solid angle. The integral is most easily carried out in terms of coordinates describing the defining slit and counter and the result is conveniently expressed as a series expansion:

$$N=\frac{d\sigma}{d\Omega_L}N_\gamma N_T\frac{ahw}{lc\sin\theta}(1+\alpha+\cdots), \tag{2}$$

where a and h are the width and height of counter 3, w is the width of the tungsten slit, c is the distance from counter 3 to the point where the axis of the telescope intersects the axis of the beam, and l is the distance between counter 3 and the slits. The term α involves squares of the ratios of a, h, w, and beam diameter to c and l and never exceeded 0.005.

The angular resolution function for the system is a symmetrical trapezoid of base $(a+w)/l$ and top $|a-w|/l$. During the course of the experiment two slit widths were employed to give differing angular resolution. However, a was nearly equal to w for both, so the resolution functions were approximately isosceles triangles. The resolution function for the range is also a trapezoid resulting from the folding of the range-interval, ΔR, with the target thickness. Since the latter was very much smaller than the former, this produced approximately a rectangle of base ΔR. Typical values of the resolution employed are indicated by the rectangles plotted in Fig. 1; the height of a rectangle indicates the proton energy interval corresponding to ΔR while its width is the half-width of the approximately triangular angular resolution. About 75% of the counting rate comes from within a rectangle.

The photon energy, k, was determined from the measured range by combining the relativistic dynamical equations relating photon and proton energy with the range-energy relation.[14]

Curves of k and $\partial k/\partial R$ *versus* R were prepared for the angles of observation employed, thus eliminating the need for any reference to proton energy in subsequent calculations. $\partial k/\partial R$ was computed from the equation $\partial k/\partial R=(\partial k/\partial E_p)(\partial E_p/\partial R)$ and used to relate the number of photons, N_γ, contributing to the observed reaction to the range-interval by means of the expressions:

$$N_\gamma=N(k)\Delta k=N(k)(\partial k/\partial R)\Delta R, \tag{3}$$

where $N(k)$ is the number of photons per unit energy in the incident bremsstrahlung spectrum.

The experiment was run almost daily for a period of three months and involved an integrated beam intensity of 10^{17} Mev. Cross sections were obtained for laboratory photon energies of 150, 200, 250, 300, 350, 400, and 450 Mev at laboratory angles of 39, 56, 74, 93, 115, and 138 degrees. A few lower-energy points were also obtained for angles in the vicinity of 90°. The energy and angular ranges accessible were limited by target geometry in the backward hemisphere and by competition from recoils involving pion production in the forward hemisphere. At each angle a complete excitation curve was obtained before moving to the next angle. Periodic checks were made which indicated that points run previously could always be reproduced within the statistical accuracy of about 5% per point. In the interest of simplicity and continuity an attempt was made to avoid too many changes in experimental conditions. Where a change was made, however, runs were overlapped to a considerable degree and this provided a valuable experimental check of the equipment. Changes in ΔR and $\Delta\theta$ produced the expected variation in counts. Changing the end-point energy of the bremsstrahlung produced discrepancies of 5 to 10% which were attributed to the production of secondary protons by mesons and higher energy nucleons in the target walls and slit jaws. The only other routine change made was the removal of counter 1 to permit access to lower energies. This produced discrepancies attributed to the production of secondary protons in the lead shielding surrounding the telescope. The effect was completely corrected by subtracting the counting rate obtained with counter 1 reinserted in anticoincidence, i.e., (1+2+3−4)=(2+3−4)−(−1+2+3−4). The production of secondaries was a principal source of trouble

[13] Johnston, Bezman, Rubin, Swanson, Corak, and Rifkin, Atomic Energy Commission Report MDDC-850 (unpublished).

[14] Aron, Hoffman, and Williams, U. S. Atomic Energy Commission Report AECU-663 (unpublished).

throughout the experiment and is discussed more fully in Sec. III.

III. EXPERIMENTAL PROCEDURE *B*

Performance of the Counter Telescope

The principal secondaries produced by high-energy bremsstrahlung are photons, electrons, mesons, neutrons, and protons. These particles incident on a single counter produce a monotonically decreasing pulse height spectrum having in general no distinguishing features whatsoever to provide orientation with respect to calibration. The problem of setting the various gains, biases, and absorbers associated with a complex telescope can, therefore, be rather slow to converge and can easily give spurious results unless a reliable systematic approach is adopted. The procedure used in the present experiment was simple and direct and led to optimum setting with a minimum of preliminary running. The first step was to observe the pulse-height spectra in the individual counters produced by a Co γ source in a standard geometry. This provided an approximate calibration and was particularly useful in periodic checks of the over-all stability of the system. Counters 3 and 4 were then connected in coincidence, (3+4), and, with the deuterium target as source, the pulse-height spectrum was observed in counter 3 with the bias on counter 4 set sufficiently high to record only heavily ionizing events. Under these conditions almost all the counts were due to protons ending near the back of counter 4 and a well-defined peak, corresponding to the ionization loss of protons of residual range, $R=C_3+A_4+C_4$, was observed in counter 3. A typical peak of this type is shown in Fig. 3–*A*; a small peak due to star-producing mesons ending in counter 4 can also be seen. The bias on counter 3 was now set just below the proton peak. We were thus certain of recording all protons of residual range, $R=C_3+A_4$, and at the same time obtaining the best possible discrimination against electrons and mesons. Note that the bias setting on counter 3 automatically includes a margin of safety due to the increase in the size of the ionization pulses when the required residual range is reduced by the thickness of counter 4. With the bias on counter 3 fixed, the bias on counter 4 was returned to a low value in the neighborhood of minimum ionization and the electronics set to record a coincidence between counters 2 and 3 accompanied by an anticoincidence in counter 4, (2+3−4). Protons could now be identified by their ionization in counter 2. The pulse-height spectrum for this counter is shown in Fig. 3–*B* and is typical of those obtained with the three-counter telescope used at low energies. Peaks corresponding to mesons and protons may be seen; the electron peak was almost entirely suppressed by the high bias on counter 3 and was not displayed in the spectrum. The relative spacing of the peaks was adjusted to give the best separation by varying the thickness of absorber 3. For the three-

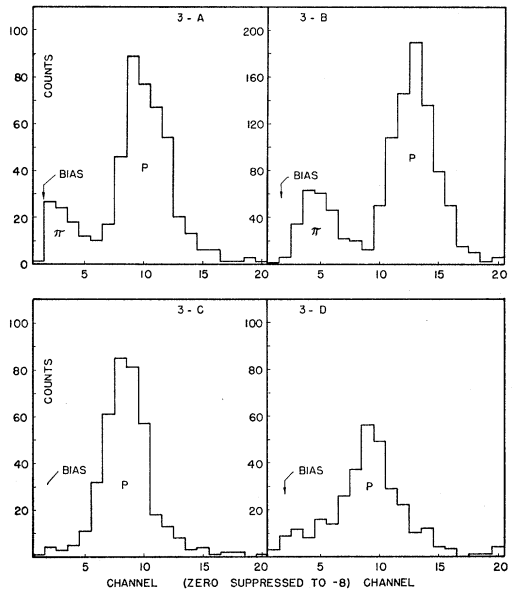

FIG. 3. Curve *A* shows a typical calibration peak for counter 3 obtained as outlined in Sec. III. Curve *B* is typical of the ionization spectra for counter 2. Curve *C* is typical of the ionization spectra for counter 1 at 39°. Curve *D* is one of the poorer spectra for counter 1 at 39°. In principle no counts should appear below the arrow marked "bias." However, the 6BN6 discriminators were slightly rate sensitive so some counts did occur in lower channels. The amplifier gain has been adjusted in each case to center the peaks. Note the suppressed zero.

counter telescope, the only remaining adjustment was to choose the thickness of absorber 2 to give the desired total range. While the system of three counters just described performs very well with respect to identification of protons, the addition of the fourth counter, C_1, was found necessary to eliminate secondary protons produced in absorber 2 and the lead shielding. A pulse height spectrum for counter 1 typical of those obtained at angles other than 39° is shown in Fig. 3–*C* while one of the poorest spectra at 39° is shown in Fig. 3–*D*. Almost no mesons are present in these spectra, because of the discrimination of a bias set between the proton and meson peaks in counter 2. The relatively poor resolution shown in Fig. 3–*D* was due primarily to electron pulses piling on top of proton pulses. This pile-up necessitated the use of a thin absorber, A_1, to shield the front counter at forward angles.

Electronics

The electronics associated with the telescope is shown by the block diagram in Fig. 4. Pulses from the RCA 5819 and Dumont 6292 photomultipliers were fed via a IN57 diode discriminator and a passive pulse-forming network into 200-ohm cables leading to amplifiers outside the beam area. The diode was biased to suppress small pulses due to electrons and permitted the use of relatively slow linear amplifiers having a rise time of 0.07 μsec without at all sacrificing the advantage of the intrinsic speed of the scintillator-photomulti-

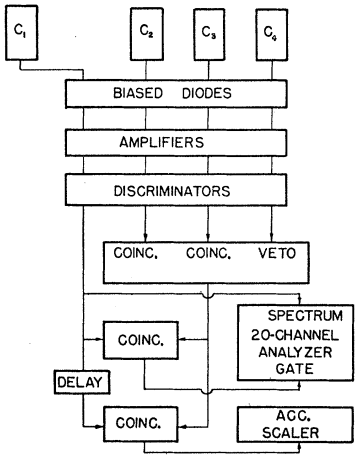

FIG. 4. Block diagram of electronics. Monitor scalers on all counters have been omitted.

plier combination with respect to pile-up. The outputs of the amplifiers were fed to 6BN6 discriminators which produced standard pulses of 0.2-μsec duration. Coincidences and anticoincidences among these pulses were formed in a simple cathode-coupled circuit having switches which permitted the function of any channel to be selected as "coincidence" or "anticoincidence." This feature was especially convenient in setting up the telescope. Provision was also made for recording various delayed coincidences used to monitor accidental and dead-time losses. The output of the coincidence unit gated a 20-channel differential pulse-height analyzer which could be used to record the spectrum of any selected counter.

ΔR Determination

Since the measured counting rates are proportional to the range-interval defined by the telescope, it is important that this parameter be as stable and well determined as possible. The exact expression for the range-interval is $R=C_3+A_4-R(E_3)+R(E_4)$. This differs from the approximate expression previously given by the terms $R(E_3)$ and $R(E_4)$ which represent the ranges in counters 3 and 4 required for the energy loss of a proton to exceed the counter biases E_3 and E_4. Since $R(E_3)$ and $R(E_4)$ are difficult to determine precisely and moreover fluctuate with the biases, it is desirable to keep them as small as possible. In practice $R(E_4)/C_3$ was about 0.03 ± 0.01 while $R(E_3)/C_3$ was about 0.08 ± 0.03. This implies an uncertainty in $-R(E_3)+R(E_4)$ of $\pm0.04C_3$. Compared to this the uncertainty in C_3+A_4 is negligible, which means an uncertainty in ΔR of approximately $4C_3/(C_3+A_4)$ percent.

An experimental check on the calculated value of the quantity $C_3-R(E_3)+R(E_4)$ was obtained by measuring the counting rate as a function of the thickness of absorber 4 and extrapolating to zero. The results are shown in Fig. 5. The straight line was fitted to the experimental points by the method of least squares. The value for $C_3-R(E_3)+R(E_4)$ obtained from the intercept was 0.114 ± 0.005 g/cm^2 Cu which agrees perfectly with the calculated value of 0.115 ± 0.004 g/cm^2 Cu.

Secondary Protons

The most important source of background encountered in the experiment was the production of secondary protons by pions and neutrons in absorber 2 and the lead shielding surrounding the counters. The magnitude of the effect at 74° may be judged from the (2+3−4) to (1+2+3−4) ratio which increased from 1.2 to 2.2 as the photon energy increased from 150 to 450 Mev. Since the shielding was more than sufficient to stop the most energetic protons and the introduction of counter 1 should in no way affect the number of valid counts, the difference in the counting rates was assumed to be due to the production of secondaries by long-range primaries, i.e., pions and neutrons. Considerable effort was spent in the investigation of these secondaries in an attempt to ascertain the most effective means of eliminating or correcting for them. The technique used was to veto the valid counts with counter 1 and then observe the effect of changing various parameters on the residue. Some of the 74° results are given in Fig. 6. The curve A shows that the number of secondaries does not change with the thickness of absorber 2. This supports the hypothesis of long range primaries and shows that equilibrium has been established in the interior of the lead shielding. The curve B, obtained by varying the thickness of absorber 3, shows that the range spectrum of the secondaries falls off about as R^{-1}. Unfortunately, we were unable to ascertain at all accurately the ratio of production by mesons and

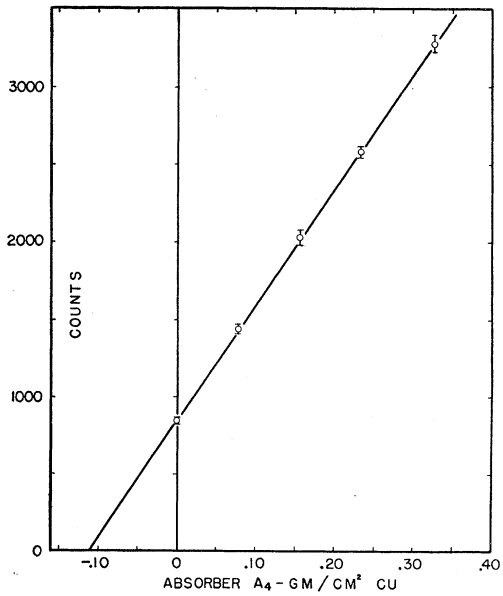

FIG. 5. Counting rate as a function of thickness of absorber 4. The straight line is a least-squares fit to points.

neutrons, although there were indications that it was about unity.

On the basis of this information, it was decided that (1) all runs possible should be made with (1+2+3−4); (2) absorber 3 should be kept as large as possible for the (2+3−4) runs used to obtain the lowest energies; (3) runs made with (2+3−4) could be corrected to yield an equivalent (1+2+3−4) result by subtracting off the counting rate (−1+2+3−4); and (4) backgrounds run with hydrogen in the target would be useful for correcting the residual effects due to pions absorbed in the target walls and slit jaws.

IV. ANALYSIS AND CORRECTION OF MEASUREMENTS

In order to ascertain the "true" number of the recoil protons resulting from photodissociation of the deuteron, the experimental observations were combined and corrected as outlined in this section.

Preliminary Adjustments

The number of proton counts in each run was determined by summing the observed pulse-height spectrum over the peak corresponding to protons, between limits chosen to estimate as well as possible the effect of overlapping tails. Using information obtained in the delayed coincidence channel, corrections were made for accidental counts and deadtime losses. Only in isolated cases did these corrections exceed 5% and, in general, they were much less. Following this all runs were adjusted for fluctuations in the beam monitor sensitivity and normalized to the same gas density. The former adjustment involved measurements of the room temperature and pressure and the bremsstrahlung end point, while the latter normalization involved measurements of the target temperature and pressure. A combined error of ±2% was assigned to these adjustments. Finally, runs made with (2+3−4) were corrected to produce equivalent (1+2+3−4) results by subtracting runs made with (−1+2+3−4). In cases of overlap, this produced agreement with actual (1+2+3−4) results. At other energies the fraction of secondaries never exceeded 20%.

Backgrounds

Backgrounds run with the target evacuated were zero to an accuracy of 1%. Backgrounds run with hydrogen as the target were, in general, less than 7%, but ranged up to 15% for 450 Mev at 38°. It was felt that subtracting these should correct for all spurious counts associated in any way with a primary process involving the proton in the deuteron.

Correction for π^- Secondaries

It is probable that the background of protons observed with hydrogen as the target was associated with the production of secondaries in the target wall and slit jaws by positive pions captured in flight. This implies an additional correction for a deuterium target due to the absorption of the negative pions produced by the neutron. From data on star production in photographic plates,[15] it was estimated that the ratio of fast protons produced in the capture of negative and positive pions was about 0.3. This factor was combined with an average minus-to-plus ratio of 1.2[16] and the measured hydrogen backgrounds to produce an estimated background associated with the neutron in the deuteron. The correction ranged from 3 to 6% and an error equal to the correction was assigned.

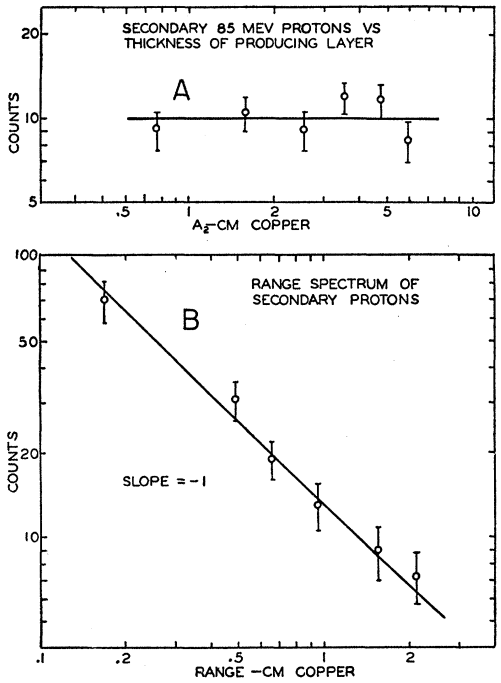

FIG. 6. Curve *A* shows the number of 85-Mev secondary protons identified in counter 2 as a function of thickness of absorber 2. Curve *B* shows the number of protons identified in counter 2 as a function of their residual range.

Correction for Scattering

The counts lost due to Coulomb and shadow scattering in the absorbers were calculated and subtracted. This correction was less than 1% except at 38° where it ranged up to 4% for the thickest value of absorber 1 employed. An error equal to half the correction was assigned. Scattering in the lead shielding and bomb wall was negligible; scattering in the slit jaws is considered below.

Correction for Nuclear Absorption

The largest single correction to the data was that due to the loss of protons in inelastic nuclear collisions in

[15] G. Bernardini and F. Levy, Phys. Rev. **84**, 610 (1951); Blau, Oliver, and Smith, Phys. Rev. **91**, 949 (1953).
[16] Sands, Teasdale, and Walker, Phys. Rev. **95**, 592 (1954).

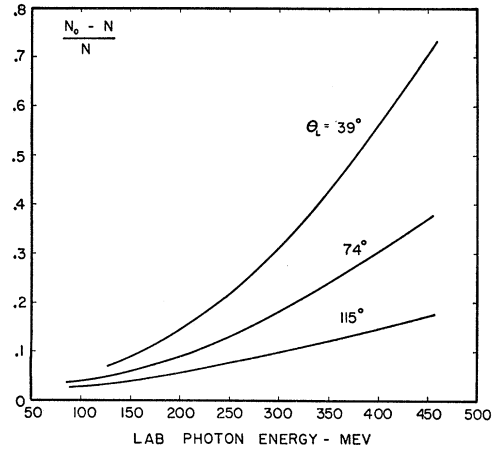

FIG. 7. Absorption correction: Ratio of counts suffering inelastic collisions in absorber 2 to counts recorded.

absorber 2. In anticipation of this, the telescope was designed to approximate the "poor geometry" used in measurements of the absorption cross section for high-energy nucleons.[17] The correction factor, N_0/N, was calculated from the relation:

$$N_0/N = \exp\left\{\int_0^R \lambda_a^{-1} dx\right\}, \qquad (4)$$

where N_0 is the original number of protons, N is the number surviving to the end of their range, and λ_a is the absorption mean free path given as a function of residual range. The theory of the transparent nucleus[18] was used to interpolate between experimental values of λ_a. The integral was computed using the empirical expression $\lambda_a^{-1} = \lambda_g^{-1}(0.84 - 0.04 \ln R)$ which is approximately correct for $0.5 < R < 10$ cm Cu. λ_g was taken as 12.4 cm for Cu. Although the absorption correction is a function only of range, it is shown in Fig. 7 as a function of photon energy and proton angle to show its magnitude at various points. For an assumed error of 5% in λ_a, the uncertainty introduced here is approximately 6% of the correction.

Correction for Degraded Protons

The most difficult corrections to calculate absolutely were those due to scattering and penetration of the slit jaws and the production of secondaries by neutrons and protons of higher energy than the protons being observed. Since an energy loss is associated with each of these effects, it was expected that they should give rise to corrections which were zero for observations made at the bremsstrahlung end point and increased as the energy of observation decreased. Estimates of the individual corrections showed them to be of equal magnitude and some place in the neighborhood of 2% for points run at 250-Mev photon energy with 500-Mev bremsstrahlung. This implied a total correction of perhaps 8% known only to within a factor of 2. Therefore, it was decided to use the calculated energy and

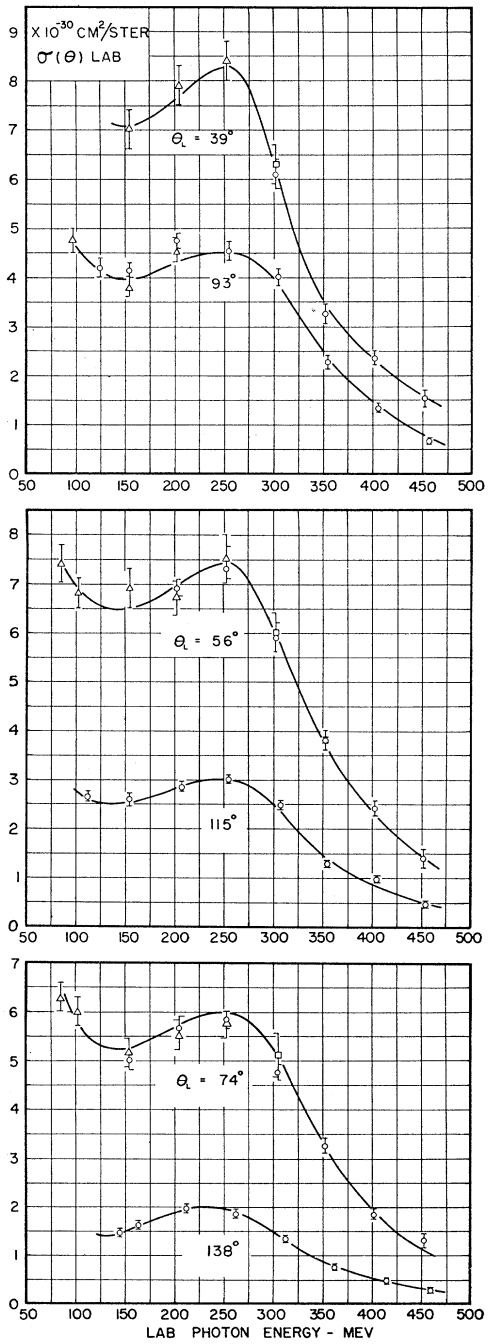

FIG. 8. Laboratory differential cross sections as a function of laboratory photon energy. Errors are standard deviations due to counting statistics and fluctuating errors only. The ○, □, and △ denote points run with 500, 400 and 300 Mev bremsstrahlung, respectively. The curves are a reconstruction of $A + B\cos\theta + C\cos^2\theta$ using coefficients from Table II.

[17] J. DeJuren and N. Knable, Phys. Rev. **77**, 606 (1950); Bernardini, Booth, and Lindenbaum, Phys. Rev. **85**, 826 (1952); William Paul Ball, University of California Radiation Laboratory Report UCRL-1938, 1952 (unpublished).

[18] Fernbach, Serber, and Taylor, Phys. Rev. **75**, 1352 (1949).

TABLE I. Center-of-momentum differential cross sections and corresponding center-of-momentum angles for photodissociation of the deuteron as a function of laboratory angle and laboratory energy. Errors given are standard deviations due to counting statistics and fluctuating errors only (units: θ_c, degrees; $d\sigma/d\Omega_c$, 10^{-30} cm^2/sterad).

θ_L	39°		56°		74°		93°		115°		138°	
K_L Mev	θ_c	$d\sigma/d\Omega_c$	θ_c	$d\sigma/d\Omega_c$	θ_c	$d\sigma/d\Omega_c$	θ_c	$d\sigma/d\Omega_c$	θ_c	$d\sigma/d\Omega_c$	θ_c	$d\sigma/d\Omega_c$
105			64.0	5.70±0.26	83.0	5.50±0.31	102.5	4.70±0.27	123.5	3.12±0.18		
155	46.5	5.25±0.31	65.5	5.61±0.37	85.0	4.64±0.21	104.5	4.14±0.17	125.5	3.16±0.16	145.5	2.15±0.10
205	47.5	5.66±0.29	67.0	5.42±0.25	87.0	5.10±0.21	106.5	4.92±0.20	127.0	3.58±0.14	146.5	2.85±0.12
255	48.5	5.85±0.32	68.5	5.76±0.25	88.5	5.27±0.21	108.0	4.86±0.19	128.5	3.90±0.15	147.5	2.93±0.14
305	49.5	4.14±0.20	70.0	4.48±0.26	90.0	4.35±0.17	109.5	4.32±0.19	129.5	3.41±0.13	148.5	2.38±0.15
355	50.5	2.09±0.14	71.0	2.78±0.14	91.0	2.82±0.12	110.5	2.48±0.13	130.5	1.79±0.10	149.5	1.38±0.11
405	51.5	1.47±0.10	72.0	1.76±0.11	92.0	1.61±0.08	111.5	1.48±0.10	131.5	1.39±0.08	150.0	0.91±0.11
455	52.0	0.93±0.11	73.0	0.99±0.16	93.5	1.15±0.12	113.0	0.76±0.07	132.5	0.68±0.07	151.0	0.52±0.12

angular dependence and fix the absolute value by requiring agreement between overlapping points obtained for 300- and 500-Mev bremsstrahlung. This involved making a least-squares adjustment of 2 parameters using 7 observations and resulted in a very satisfactory meshing of the points. The correction was largest, 15%, for 300-Mev at 38° and tapered to a few percent with increasing angle or energy. Where there were points obtained with 300-Mev bremsstrahlung, these were considered correct. For all other points an error of approximately half the correction was assigned.

Other Corrections

The correction for recoils associated with pion production was estimated for the "spectator" process.[10] In the absence of a specific effect which might favor the recoil of a meson and nucleon in the same direction, "apron-string" process, it was found to be negligible for all the points used in the final analysis. Some experimental evidence that the "apron-string" process was not too important for this experiment was provided by a failure to detect a component having an appropriate dependence on angle and energy in the discrepancy between runs with 300 and 500-Mev bremsstrahlung.

Finally, the number of dissociations induced by the absorption of positive pions in the deuterium[19] was estimated and found to be $\lesssim 0.1\%$. This was fortunate since, for relativistic pions produced at small angles, the dynamics of this two-step process are virtually identical to those for true photodissociation.

V. SUMMARY OF RESULTS

The laboratory differential cross sections for photodissociation of the deuteron were calculated from Eq. 2 of Sec. II using the "true" counting rates obtained by the method described in Sec. IV. The results are shown in Fig. 8 plotted as a function of laboratory photon energy for the various laboratory angles investigated. The errors indicated are standard deviations obtained by combining the counting statistics with fluctuating errors associated with monitor sensitivity and density determinations. In addition, there are two other types of error which are not shown. The first is an 8% error in the absolute value of the cross sections due primarily to the 7% uncertainty in beam calibration but also containing estimates of uncertainties in the range interval and solid angle. The second is the error associated with the smooth corrections described in Sec. IV. This is estimated at 10% of the absorption correction and is appreciable only for the highest energies at forward angles. The curves drawn through the points are a reconstruction of an empirical expression used to fit the angular distributions as discussed below.

The differential cross sections in the center-of-momentum system are listed in Table I and plotted in Fig. 9 as a function of angle for various laboratory photon energies. They were obtained from the laboratory excitation curves by first making a linear interpolation between the experimental points to obtain cross sections at a common photon energy, and then applying the solid angle transformation. The errors shown are the same as those on the excitation curves. In order to obtain total cross sections and facilitate comparison with other experiments, empirical curves of the form $A+B\cos\theta+C\cos^2\theta$ were fitted to the data by the method of least squares. The form assumed has no theoretical justification and, indeed, does not even have the correct asymptotic behavior at low energies, i.e., $A+B\sin^2\theta(1+2\beta\cos\theta)$. However, it has the practical advantage of fitting the data better than other simple forms having only three parameters. The values

TABLE II. The coefficients A, B, and C are those obtained by a least-squares fit of the empirical expression $A+B\cos\theta+C\cos^2\theta$ to the data in Table I and published Cornell data. The total cross-sections were computed from the expression $\sigma_T=4\pi(A+\frac{1}{3}C)$ obtained by integration of $A+B\cos\theta+C\cos^2\theta$ with respect to solid angle. In addition to the errors shown there are quoted uncertainties of about 10% in the absolute value scales (units: A, B, and C 10^{-30} cm^2/sterad; σ_T, 10^{-30} cm^2).

Laboratory	K_L Mev	A	B	C	σ_T
CalTech	105	5.30±0.23	2.08±0.36	−2.4 ±1.2	57 ±4
	155	4.68±0.13	1.90±0.22	−1.39±0.35	53.1±1.4
	205	5.16±0.13	1.54±0.20	−1.51±0.36	58.6±1.2
	255	5.40±0.13	1.55±0.22	−1.56±0.39	61.4±1.3
	305	4.57±0.12	0.61±0.17	−2.15±0.32	48.3±1.1
	355	2.79±0.08	0.19±0.12	−1.81±0.23	27.6±0.7
	405	1.68±0.06	0.14±0.10	−0.73±0.18	18.1±0.6
	455	0.98±0.07	0.20±0.10	−0.41±0.20	10.6±0.6
Cornell	180	4.42±0.15	1.61±0.22	−0.51±0.42	53.5±1.4
	260	5.56±0.21	1.62±0.24	−1.29±0.49	64.5±1.7

[19] Durbin, Loar, and Steinberger, Phys. Rev. **84**, 581 (1951); Henry L. Stadler, Phys. Rev. **96**, 496 (1954).

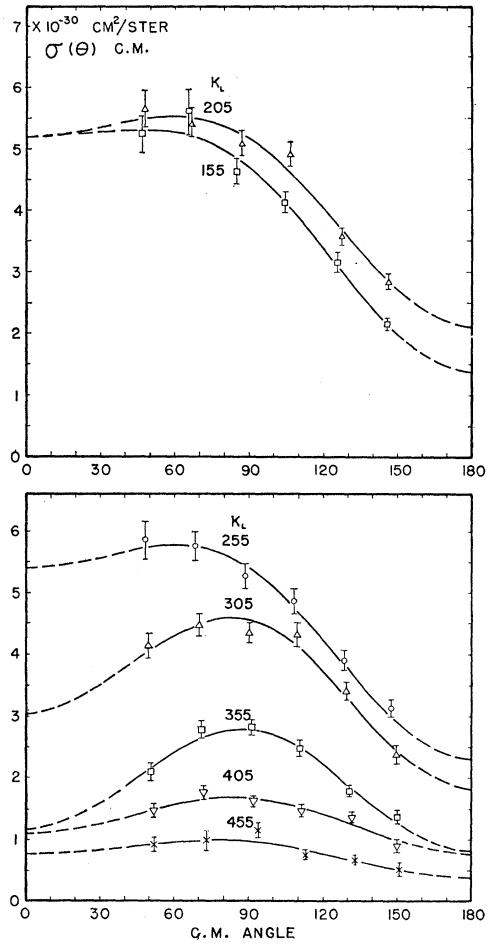

FIG. 9. Center-of-momentum differential cross sections as a function of center-of-momentum angles. Errors are the same as for Fig. 8 The curves are a reconstruction of $A+B\cos\theta+C\cos^2\theta$ using coefficients from Table II.

for A, B, and C are tabulated in Table II. The curves in Figs. 8 and 9 are all reconstructions using these coefficients. Also given in Table II are values of A, B, and C obtained by fitting Cornell[9] data.

Total cross sections as a function of laboratory photon energy are listed in Table II and plotted in Fig. 10. These were calculated from the equation $\sigma_T=4\pi(A+\frac{1}{3}C)$ obtained by integrating $A+B\cos\theta+C\cos^2\theta$ with respect to solid angle. The errors assigned take into account the fact that errors in A and C are correlated.

VII. DISCUSSION OF RESULTS AND COMPARISON WITH THEORY

As may be seen in Fig. 10, the total cross sections measured in this experiment agree well with those reported by Cornell[9] and Illinois.[20] There is also satisfactory agreement with regard to the angular distributions. This is shown in Fig. 11 where the values of the coefficients B/A and C/A obtained by fitting the data with the emprical curve $1+(B/A)\cos\theta(C/A)\cos^2\theta$ are compared. The CalTech and Cornell points come from Table II and carry errors given by the least squares analysis. It is probably reasonable to assume that the errors in the Illinois[20] points are comparable.

The principal features of the process in the high-energy region established by these experiments are summarized here. Above 100 Mev, the total cross section is more than 5 times that calculated for electric interactions[21] and exhibits a relative minimum at 150 Mev followed by a relative maximum at 250 Mev. This rather striking behavior may be compared with the existence of resonance maxima in the photopion cross sections[22] and indicates that meson phenomena play an important role in the interaction. The center-of-momentum angular distributions, which are essentially $\sin^2\theta$ at low energies, show a large isotropic component above 100 Mev and a strong forward maximum which suggests a considerably larger cross section at 0° than at 180°. As will be seen later, this asymmetry is the feature most difficult to reconcile with theory. Above 250 Mev the isotropic component persists, but the asymmetry diminishes until at the highest energies the angular distributions are again consistent with symmetry about 90°.

In the low-energy limit, it is expected that an adequate theoretical description of the photodissociation

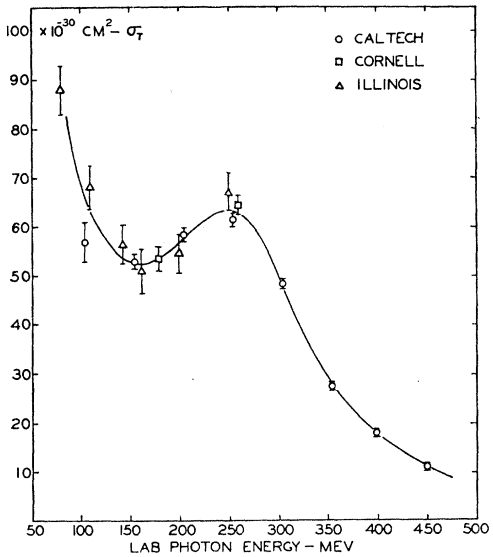

FIG. 10. Total cross sections for photodissociation of the deuteron as a function of laboratory energy. The CalTech and Cornell cross sections were taken from Table II and are subject to a quoted uncertainty of 10% in absolute value. The Illinois data were kindly communicated to the authors by A. O. Hanson. The solid curve is drawn through the experimental points.

[20] Experiments of reference 8 summarized by A. O. Hanson (private communication).

[21] L. I. Schiff, Phys. Rev. 78, 733 (1951); J. F. Marshall and E. Guth, Phys. Rev. 78, 738 (1950).

[22] California Institute of Technology experiments on pion production in H and D.

of the deuteron should be possible without explicit reference to the meson fields through which the nucleons interact[23] and, indeed, good agreement with experiment is obtained up to about 10 Mev.[1] From 20 to 60 Mev the total cross sections are still in reasonable agreement with experiment,[8] but departures are noted in the angular distributions. The experiments indicate a growing isotropic component while calculations[21] of the dominant electric dipole and quadrupole transitions from the ^3S state assuming a central potential give zero cross sections at 0° and 180°. A number of explanations of this isotropic component have been advanced. These involve consideration of ordinary magnetic transitions,[21,24] tensor forces,[25] and transitions from the ^3D state.[24] While the results show promise of being able to explain the experiments, all authors point out the probable importance, particularly for magnetic interactions, of specific meson effects which have been neglected. In view of the manifest importance of meson interaction at higher energies, it seems probable that this neglect is unjustified and that even below 60 Mev the influence of mesons must be considered.[26]

For energies in excess of 100 Mev, only the meson theories give even qualitative agreement with experiment. One of the first estimates of the total cross section based explicitly on the meson interactions was made by Wilson.[5] Following a suggestion due to Fermi,[27] he argued that, if the deuteron absorbed a photon at a time when its constituent nucleons were within the range of nuclear forces, a statistical equilibrium might be established in which phase-space factors would essentially determine the relative probabilities for dissociation or pion production. With the further assumption that the cross section for the absorption of a photon by a nucleon is not appreciably altered by the proximity of another nucleon, he was able to estimate a contribution to the total cross section for photodissociation by simply multiplying the sum of the photomeson cross sections for the free constituent nucleons by the probability of finding them within a distance $\hbar/mc$ in the deuteron. This procedure led to results in approximate agreement with experiment and gave promise of success to be achieved by the application of meson theory to the problem.

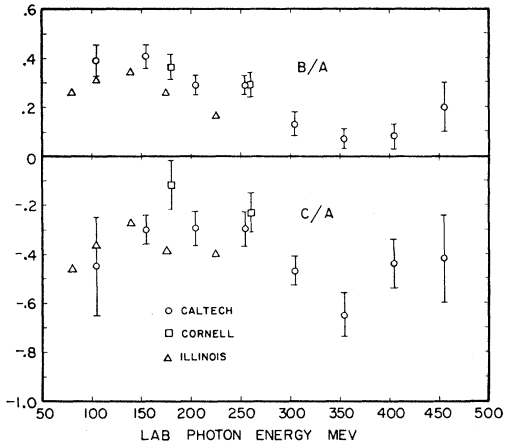

FIG. 11. Coefficients obtained by fitting CalTech, Cornell, and Illinois angular distributions with the empirical expression $(1+(B/A)\cos\theta+(C/A)\cos^2\theta)$. The CalTech and Cornell points are taken from Table II. The Illinois data were kindly communicated to the authors by A. O. Hanson.

More sophisticated calculations have now been made by a number of authors. Nagahara and Fujimura[28] have calculated the dipole transitions due to exchange currents using an operator taken from pseudo-scalar meson theory. Their results for the total cross section show rough agreement with the experiments up to 250 Mev but have not been carried over the maximum in the cross section. An extension of the calculations by Fujimura[29] gives angular distributions which are roughly isotropic and, therefore, do not agree with present observations.

Calculations using pseudoscalar meson theory in lowest order have also been made by Bruno and Depken.[30] They find reasonable agreement for the total cross section up to about 100 Mev, but their cross section decreases monotonically with energy and thus is seriously in error at higher energies.

Austern[31] has investigated a model in which he assumes as an intermediate step in the process the excitation of an isobaric state $(\frac{3}{2},\frac{3}{2})$ of a nucleon. This model gives angular distributions of the simple form $(1+\frac{3}{2}\sin^2\theta)$, which could be consistent with the observations at the highest energies but is in disagreement at lower energies. He is currently extending his calculations to give total cross sections as a function of energy.

A tentative phenomenological treatment has been given by Watson.[32] This work is an extension of the theory of photopions[33] in which dissociation of the deuteron results from the production of a (virtual) pion on one nucleon and its subsequent reabsorption in a Chew-type[34] interaction by the other. The theory should include on a phenomenological level all the effects

[23] A. F. J. Seigert, Phys. Rev. **52**, 787 (1937); R. G. Sachs and N. Austern, Phys. Rev. **81**, 705 (1951); J. G. Brennan and R. G. Sachs, Phys. Rev. **88**, 824 (1952); L. L. Foldy, Phys. Rev. **92**, 178 (1953).
[24] Yoshio Yamaguchi, Phys. Rev. **95**, 1628 (1954); Y. Yamaguchi and Y. Yamaguchi, Phys. Rev. **95**, 1635 (1954).
[25] W. Rarita and J. Schwinger, Phys. Rev. **59**, 556 (1951); T. Hu and H. S. W. Massey, Proc. Roy. Soc. (London) **A196**, 135 (1936); N. Austern, Phys. Rev. **85**, 283 (1952).
[26] J. M. Berger, Phys. Rev. **94**, 1698 (1954).
[27] E. Fermi, Progr. Theoet. Phys. (Japan) **5**, 570 (1950).
[28] Y. Nagahara and J. Fujimura, Progr. Theoret. Phys. (Japan) **8**, 49 (1952).
[29] Jun Fujimura, Progr. Theoret. Phys. (Japan) **9**, 132 (1953).
[30] B. Bruno and S. Depken, Arkiv Fysik **6**, 177 (1953).
[31] N. Austern, Phys. Rev. **85**, 283 (1952) and private communication.
[32] K. M. Watson (private communication).
[33] M. Gell-Mann and K. M. Watson Ann. Revs. Nuclear Sci. **4**, 219 (1954) and private communication.
[34] G. F. Chew, Phys. Rev. **94**, 1748, 1755 (1954).

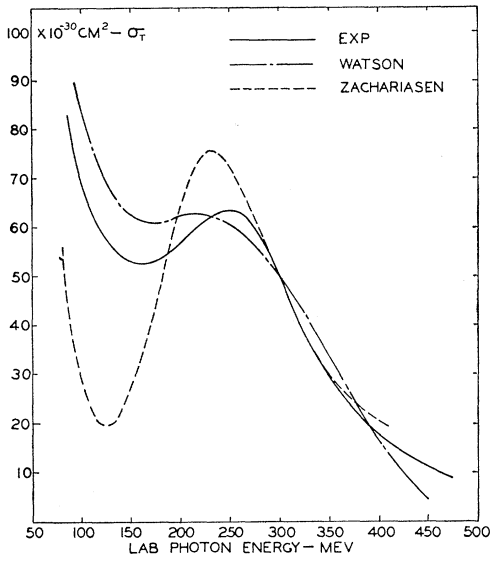

FIG. 12. Comparison of the experimental and theoretical total cross sections for photodissociation of the deuteron. The solid curve is that shown in Fig. 10 and represents the experimental results. The broken curve is that given by Watson's phenomenological calculation. The dashed curve is that given by Zachariasen's calculation.

considered by the authors previously mentioned. The theory contains one parameter which in principle could be calculated but which at present is regarded as adjustable. The total cross section is in qualitative agreement with experiment, as can be seen in Fig. 12. The angular distributions fail to have sufficiently strong forward maxima between 100 and 250 Mev, although reasonable agreement is achieved at higher energies.

The most logically complete calculation has been made recently by Zachariasen.[35] His approach to the problem was to set up, first, a formally correct expression for the matrix element involved. He then extracted the principal terms and evaluated them, using the Chew formalism.[34] In addition to terms involving the photoproduction of mesons on one nucleon and subsequent reabsorption by the other, as in the Watson theory, Zachariasen finds an important term corresponding to the S-wave production of a meson on one nucleon which scatters in the resonant $(\frac{3}{2}, \frac{3}{2})$ state on the other nucleon and is then reabsorbed by the original nucleon. This term, which interferes destructively with other terms, leads to a pronounced minimum in the total cross section at 125 Mev. As may be seen by Fig. 12, this feature is not too well borne out experimentally, but in other respects there is reasonable agreement. Unfortunately, in common with other theories, the angular distributions fail to show the strong forward maxima. However, Zachariasen feels that his angular distributions may be unreliable due to the neglect of terms which, though unimportant for the total cross section, might produce appreciable interference effects.

Although the detailed comparison with theory is still far from satisfactory, considerable progress has been made and we may hope that with further study the situation will improve. In view of the special difficulty encountered in explaining the angular distributions, it would be most desirable to extend the experimental observations to 0° and 180°.

[35] Fredrik Zachariasen, Thesis California Institute of Technology 1955 (unpublished); see also F. Zachariasen, following paper [Phys. Rev. **101**, 371 (1956)].

ACKNOWLEDGMENTS

The authors wish to acknowledge the help and support of all members of the synchrotron laboratory during the course of this experiment. We are particularly indebted to Mr. R. W. Smythe II, who participated in the early phases of the experiment, to Dr. A. O. Hanson for communication of Illinois results, and to Dr. R. F. Bacher for encouragement and critical discussion of the results. Dr. R. V. Langmuir, Dr. M. Sands, Dr. J. G. Teasdale, Dr. R. L. Walker, and Mr. B. H. Rule assisted in running the synchrotron.